Frequency-Scalable Nonlinear-Transmission-Line-Based Vector Network Analyzers

Karam Noujeim, Jon Martens, and Tom Roberts

Microwave Measurements Division
Anritsu Co.
490 Jarvis Drive
Morgan Hill, CA 94086
USA

Tel: 408.201.1766
E-mail: Karam.Noujeim@anritsu.com

ABSTRACT - An overview of the high-frequency reflectometer technology deployed in Anritsu's VectorStar Vector Network Analyzer (VNA) family is given, leading to a detailed description of the architecture used to extend the frequency range of VectorStar into the high millimeter waves. It is shown that this technology results in miniature frequency-extension modules that provide unique capabilities such as direct connection to wafer probes, dense multi-port measurements, test-port power leveling, enhanced raw directivity, and reduced measurement complexity when compared with existing solutions. These capabilities, combined with the frequency-scalable nature of the reflectometers provide users with a unique and compelling solution for their current and future high-frequency measurement needs.

I. Introduction

High-frequency VNAs make use of harmonic samplers or mixers to down-convert measurement signals to IF frequencies before digitizing them. Such down-conversion components play a critical role in VNAs because they set bounds on important parameters like conversion efficiency, receiver compression, isolation between measurement channels, and spurious generation at the ports of a device under test (DUT). While harmonic samplers and mixers each have their own unique advantages and drawbacks, mixers tend to be the down converters of choice at RF frequencies, due mainly to their simpler local oscillator (LO) drive system and enhanced spur-management advantages. At microwave and millimeter-wave frequencies (where receiver compression and cost are of major concern), harmonic sampling is often used. In situations where the frequency band spans the RF, microwave and millimeter-wave spectra, harmonic samplers and mixers can be used in tandem to optimize performance across the entire frequency range of the VNA. This architecture is at the heart of the VectorStar [1] VNA family, and its extension into the high millimeter waves is the focus of this paper.

II. Equivalent-time sampling

Sampler-based reflectometers make use of equivalent-time sampling or harmonic mixing to 'time-stretch' coupled versions of the waves incident on, and reflected from a DUT prior to digitizing them with an analog-to-digital converter (ADC). This approach results in a simplified VNA architecture with reduced cost in comparison with one employing fundamental mixing. This is a direct result of the nature of the equivalent-time-sampling process in which the frequency range of the local oscillator (LO or strobe) is confined to an octave or so, while its harmonics effect the down-conversion of the coupled high-frequency signals as shown in Fig. 1. Consequently, the LO source required for strobing the samplers operates in a lower frequency range than that which would be required in a fundamental-mixer VNA, be it at the expense of increased conversion loss.

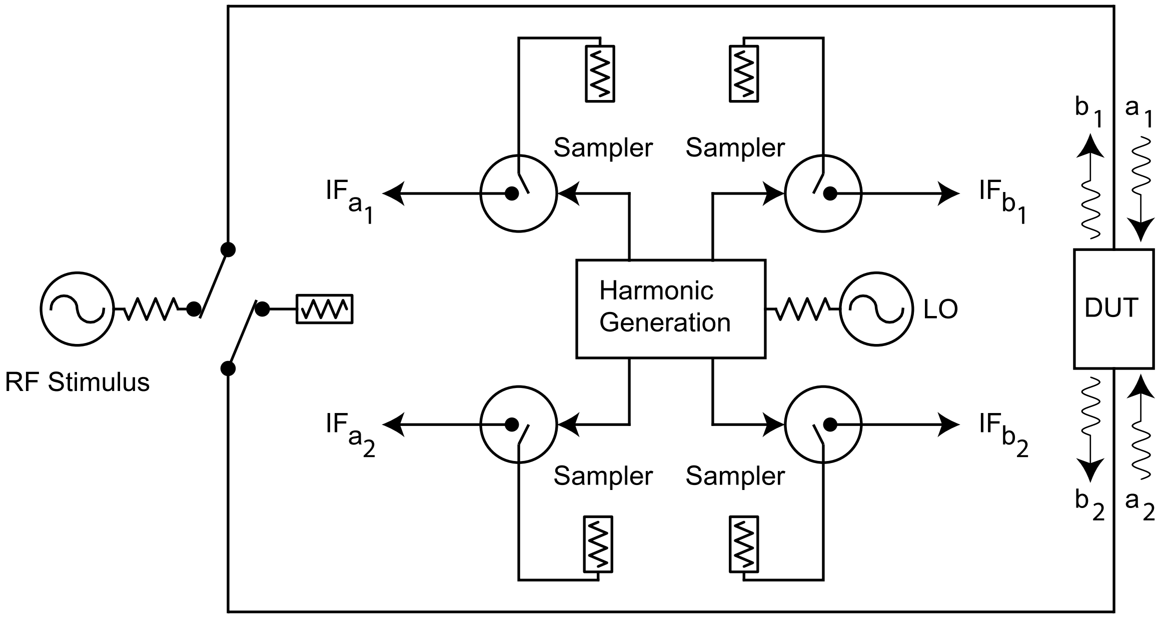

Figure 1. A VNA reflectometer architecture based on equivalent-time sampling. Samplers have traditionally been gated by pulses generated by a step-recover-diode (SRD) circuit. The LO and RF sources are synchronized.

The periodic nature of the incident and reflected waves in Fig. 1 makes their down conversion possible by means of equivalent-time sampling, also known as under-sampling, harmonic sampling, or super-Nyquist sampling. A time-domain illustration of this sampling process is shown in Fig. 2. Here, samples of a sinusoidal RF waveform of period T_{RF} appear at the output of an ideal switch gated at a rate of T_{LO}. As is evident from Fig. 2, the sampled IF waveform, $v_{IF}(t)$, is the arithmetic product of the sinusoidal RF waveform, $v_{RF}(t)$, and the ideal-switch conductance, $g(t)$. That is,

$$v_{IF}(t) = v_{RF}(t) \times g(t) \qquad (1)$$

where $g(t)$ can be expressed as a trigonometric Fourier series [2] as in (2)

$$g(t) = \frac{B \cdot T_g}{T_{LO}} + 2 \cdot \frac{B \cdot T_g}{T_{LO}} \sum_{n=1}^{\infty} \mathrm{sinc}\left(\frac{n \cdot \pi \cdot T_g}{T_{LO}}\right) \cos(2 \cdot \pi \cdot n \cdot f_{LO} \cdot t) \qquad (2)$$

where $\mathrm{sinc}(x) = \sin(x)/x$.

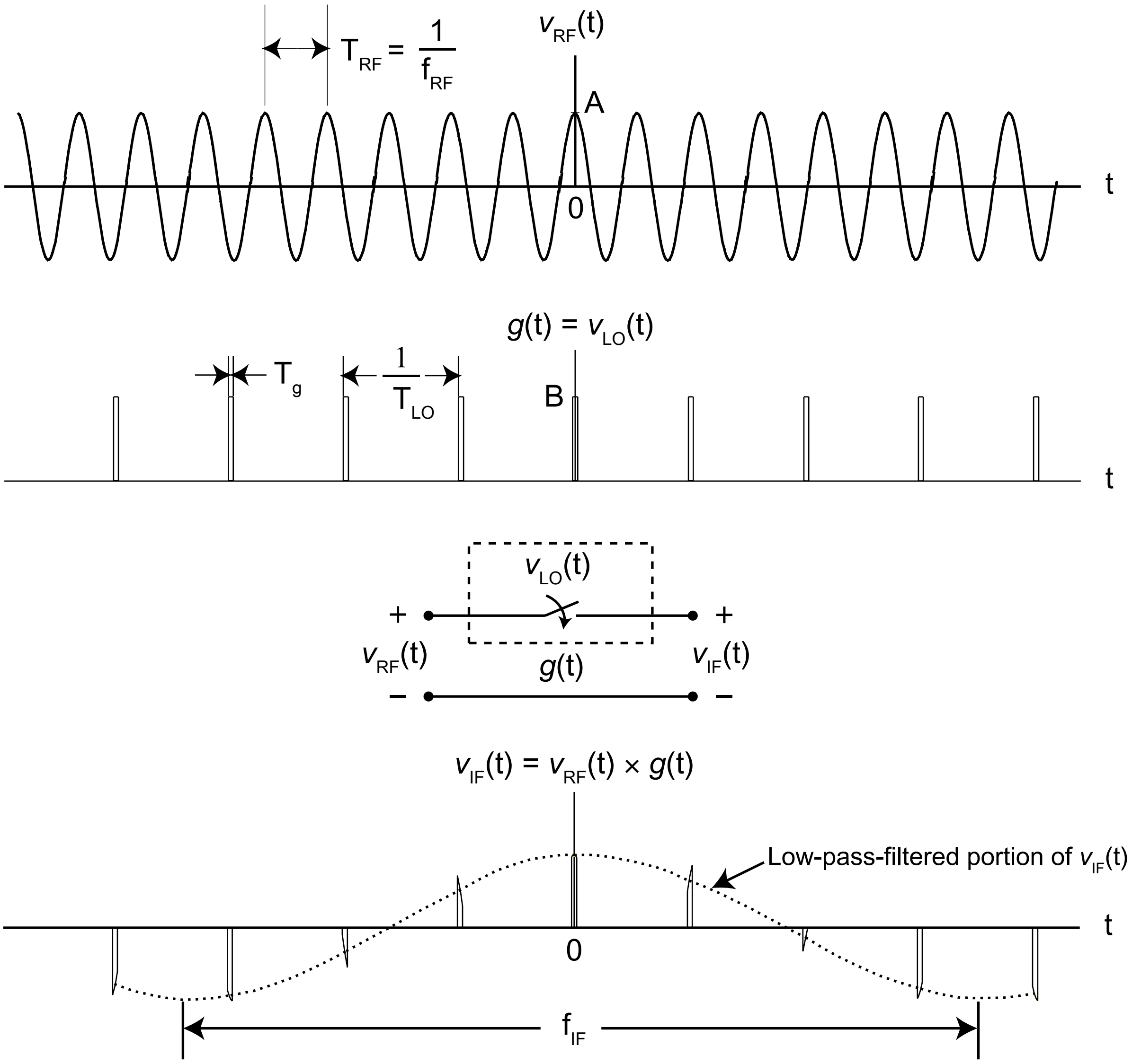

Figure 2. A time-domain illustration of equivalent-time sampling. (a) A sinusoidal RF waveform $v_{RF}(t) = A\cos(2\pi f_{RF}t,)$ appearing at the input of the ideal series switch. (b) The switch conductance, $g(t)$, with a gating aperture, T_g, and a rate of $f_{LO} = 1/T_{LO}$ (Hz). (c) The down-converted IF waveform, $v_{IF}(t)$, along with a low-pass filtered version of the same.

It is evident from Fig. 2 that low-pass filtering of the IF waveform results in a 'time-stretched' replica of the RF waveform. It can also be shown that the gating time, T_g, has a considerable effect on the magnitude response of the ideal switch. That is, reducing the gating time of the switch is accompanied by an increase in the RF bandwidth at the expense of reduced conversion efficiency.

Practical implementations of samplers for VNAs have traditionally relied on Schottky diodes as switches, and on step-recovery diodes (SRD) for pulse generation. One such implementation, a sampling circuit due to Grove [3], has been used extensively in a range of instruments, including microwave VNAs, sampling oscilloscopes, and frequency counters. In this circuit, a voltage pulse is used to gate Schottky diodes over a brief time interval, T_g, known also as the gating time. Over this interval, the Schottky diodes are driven into conduction and charge sampling capacitors, C_s. The charge present on the capacitors results in an output waveform that is related to the polarity and amplitude of the RF input.

III. Isolation between VNA test channels

While SRDs made the extension of the RF bandwidth in VNAs to 65 GHz possible [4], a limited fall time and a lack of LO frequency scalability prevent their use in higher-frequency VNAs. In addition, the dynamic range of transmission measurements in an SRD-based sampling VNA is limited by the lack of broadband devices for isolating test channels. Channel isolation is best understood by considering the SRD-gated sampling reflectometer shown in Fig. 3 and noting that suppression of leaky signals requires the use of broadband isolation devices in the output arms of the splitter. In the absence of such devices,

- Forward-transmission measurements on highly-reflective DUTs lead to increased signal-power leakage from sampler 2 to sampler 3.
- Reverse-transmission measurements on highly-reflective DUTs lead to increased signal-power leakage from sampler 3 to sampler 2.

These observations, coupled with the fact that such frequency-dependent leakage phenomena cannot be calibrated out, impose limitations on the dynamic range of an SRD-based sampling VNA. These in turn prevent the full characterization of highly reflective devices such as highpass filters, as well as devices where weak coupling among constituents must be measured fully as a function of frequency (e.g. weak crosstalk).

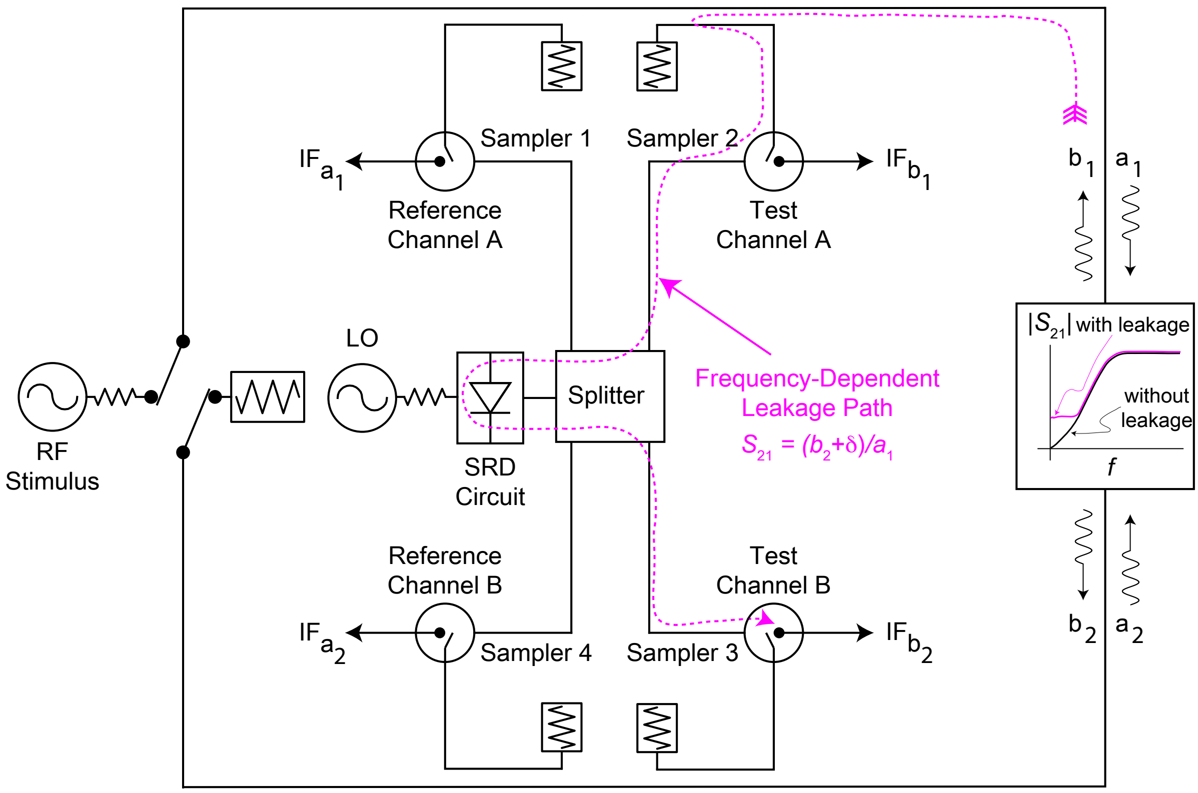

Figure 3. A sampling VNA based on a step-recovery diode (SRD). Leakage between test channels limits the VNA's dynamic range, preventing full characterization of highly reflective devices such as waveguide filters. Here, coherence among sampling channels is maintained by making use of a single SRD.

The aforementioned limitations of SRD-based sampling VNAs can be overcome by making use of samplers based on nonlinear transmission lines (NLTL). NLTLs are distributed devices that support the propagation of nonlinear electrical waves such as shock waves and solitons [5]. They are made up of high-impedance transmission lines loaded with varactor diodes so as to form a propagation medium whose phase velocity and thus, time delay, is a function of the instantaneous voltage [6]-[9]. For a step-like waveform propagating along an NLTL, the trough of the wave travels at a faster phase velocity than the peak. This results in compression of the fall time and as a result, the formation of a steep wave front that approaches that of a shock wave.

Due to their attractive features, NLTL-based samplers have been developed for use in the VectorStar VNA family. These features include RF and LO frequency scalability, as well as suitability for achieving high isolation between channels. Such isolation is key to achieving high dynamic range as noted earlier, and is carried out here by means of amplifiers as shown in Fig. 4. In the stopband of a DUT such as a highpass filter for example, and while in forward-transmission-measurement mode, a substantial amount of incident-signal power is reflected and received by test-channel A. Due to RF-LO coupling in sampler 2, a portion of the received signal power propagates along sampler 2's NLTL while undergoing loss and encounters eventually the reverse path of the amplifiers, which provides a degree of isolation. The isolation between test channels A and B may be enhanced further by adding additional amplifiers and isolators, in series, in an appropriate order. Due to the symmetry of the test channels, identical isolation components appear in test-channel B.

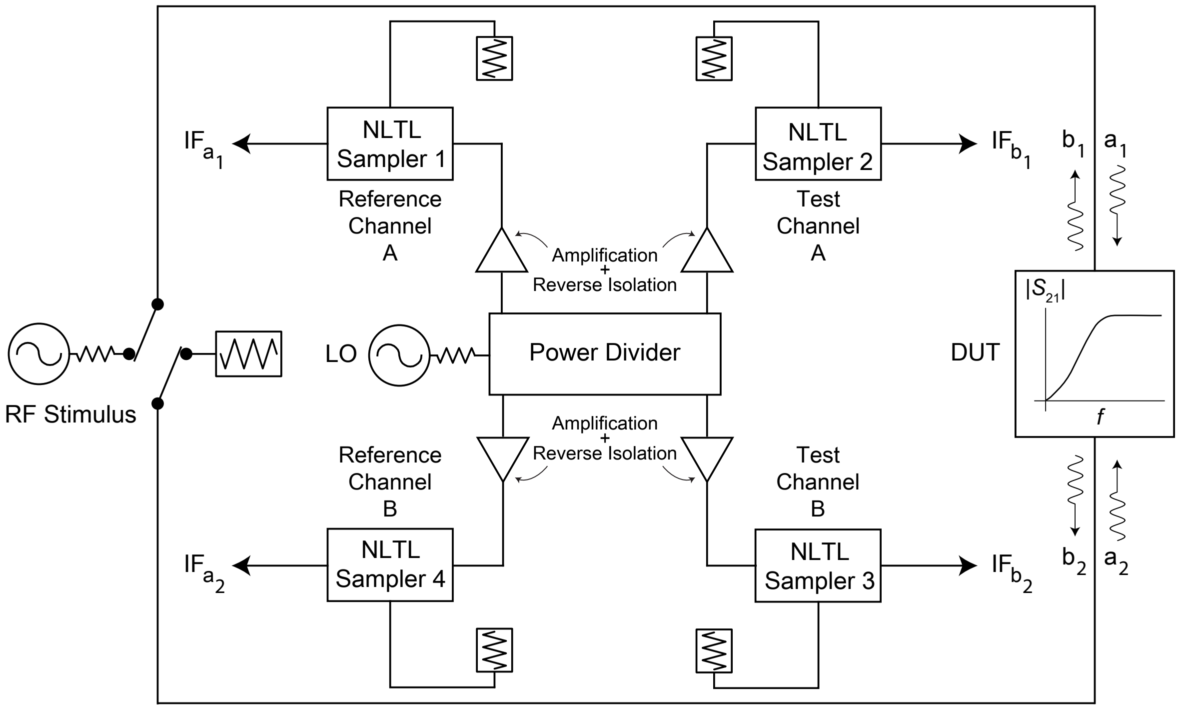

Figure 4. A sampling VNA based on nonlinear-transmission-line (NLTL) samplers. Leakage between channels is suppressed by means of isolation devices such as amplifiers and isolators.

IV. Reflectometer extensions to higher frequencies

In order to extend the bandwidth of a VectorStar VNA to 110 GHz, an external reflectometer was designed based on NLTL samplers and harmonic generators. The reflectometer was integrated with the VNA as shown in Fig. 5, illustrated here as part of a one-port setup for the sake of clarity and without loss of generality. Figure 6 shows a picture of the actual reflectometer with key characteristics summarized below.

- Small size and lightweight. These features enhance maneuverability and probe positioning in applications such as on-wafer measurements and near-field scanning of antennas and circuits.
- A continuous RF path starting in the base VNA and leading to the DUT. This allows the base VNA to provide RF stimulus from 70 KHz to 54 GHz. It also allows use of the external reflectometer receiver in the range 30–54 GHz for improving the raw directivity of the base VNA. The external reflectometer receiver and harmonic generators are used from 54 – 110 GHz.
- A vanishing thermal gradient across the reflectometer module, and thus across the sampling directional bridge for improved measurement stability.
- Automatic level control (ALC) for LO stability.
- A high-performance transition from the RF path to the 1-mm connector of the test port.
- Test-port power leveling.
- Potential for connecting the reflectometer directly (i.e. without a cable) to a wafer probe. This brings the "VNA" yet closer to the DUT, thus enhancing raw directivity and port power.

The measured raw directivity of the VNA and its external reflectometer is shown in Fig. 7, and is better than 6 dB across the entire frequency range. Raw directivity, coupled with a vanishing thermal gradient across the external reflectometer and LO level control contribute to long-term measurement stability. On the other hand, the measured dynamic range shown in Fig. 8 exceeds 100 dB from 70 KHz to 110 GHz, making possible the characterization of highly reflective devices and weak crosstalk. Finally, the measured LO power leakage out of the test port of the reflectometer is less than −40 dBm in the entire LO frequency range 5–10 GHz. This is achieved by careful design of the LO driver circuits which are isolated from the test port by at least 65 dB in the 5–10 GHz range. LO leakage could be filtered further since it is out of band.

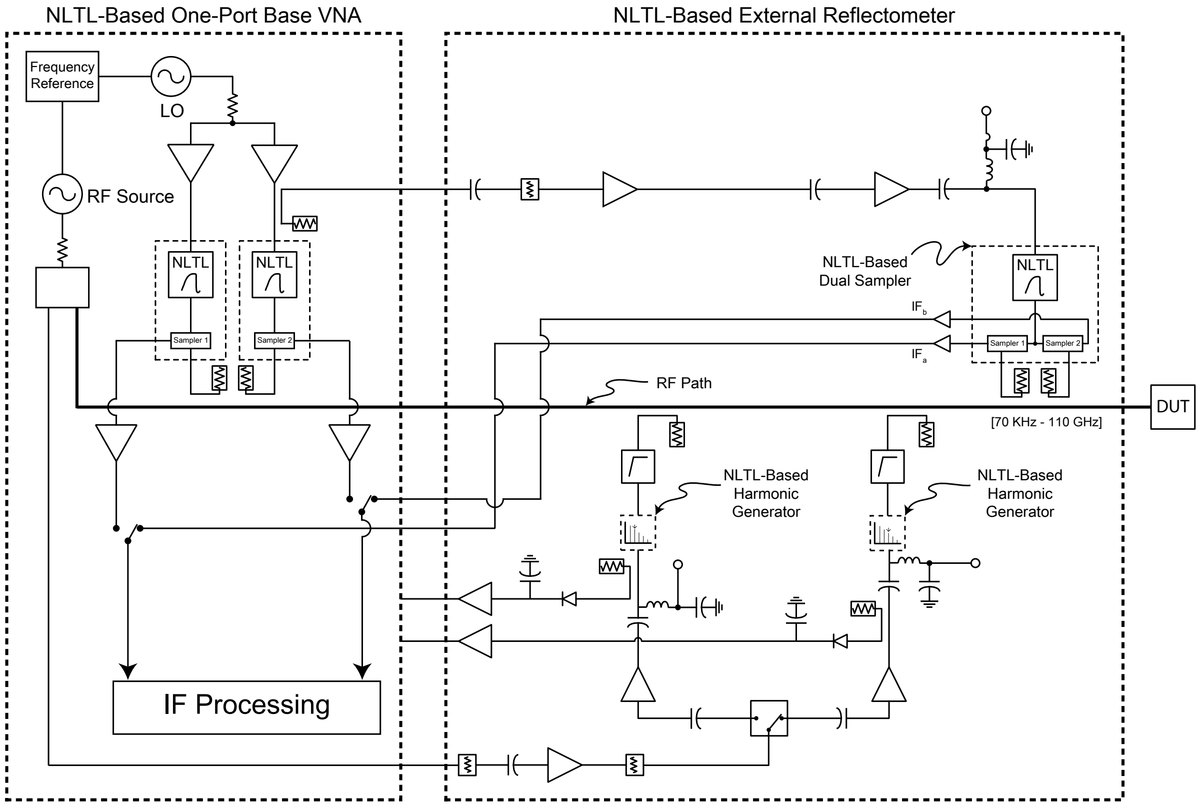

Figure 5. NLTL-based reflectometer integrated here with a one-port VNA for illustration purposes.

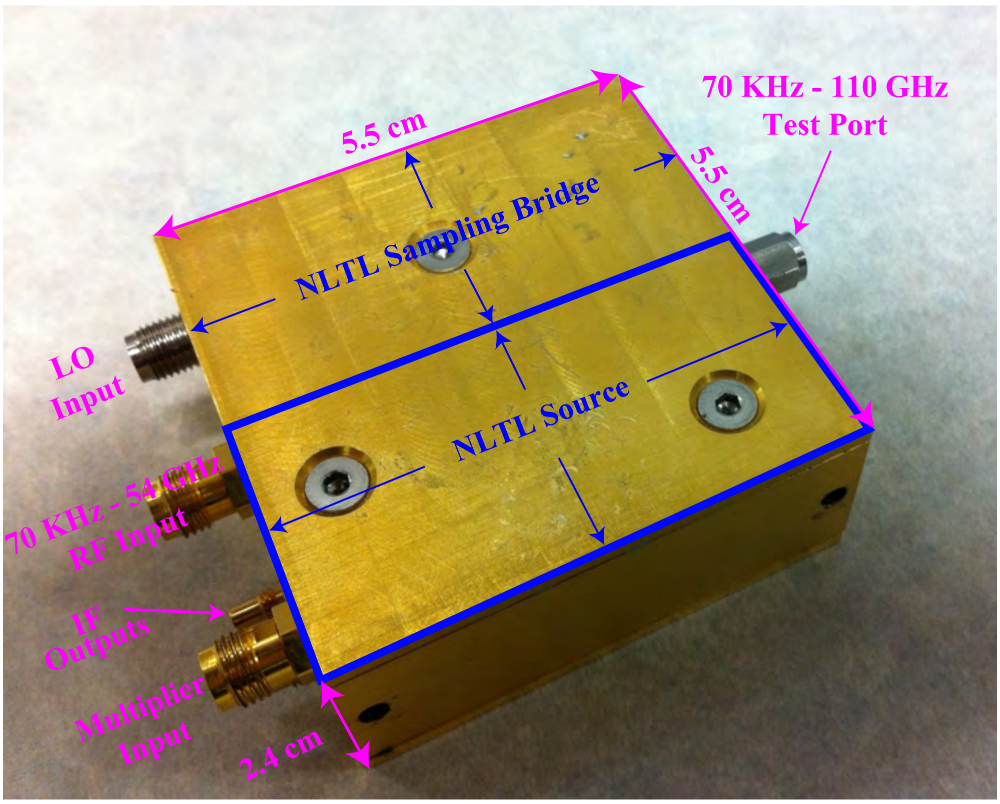

Figure 6. NLTL-based external reflectometer for extending the frequency range of a VectorStar VNA from 54 to 110 GHz.

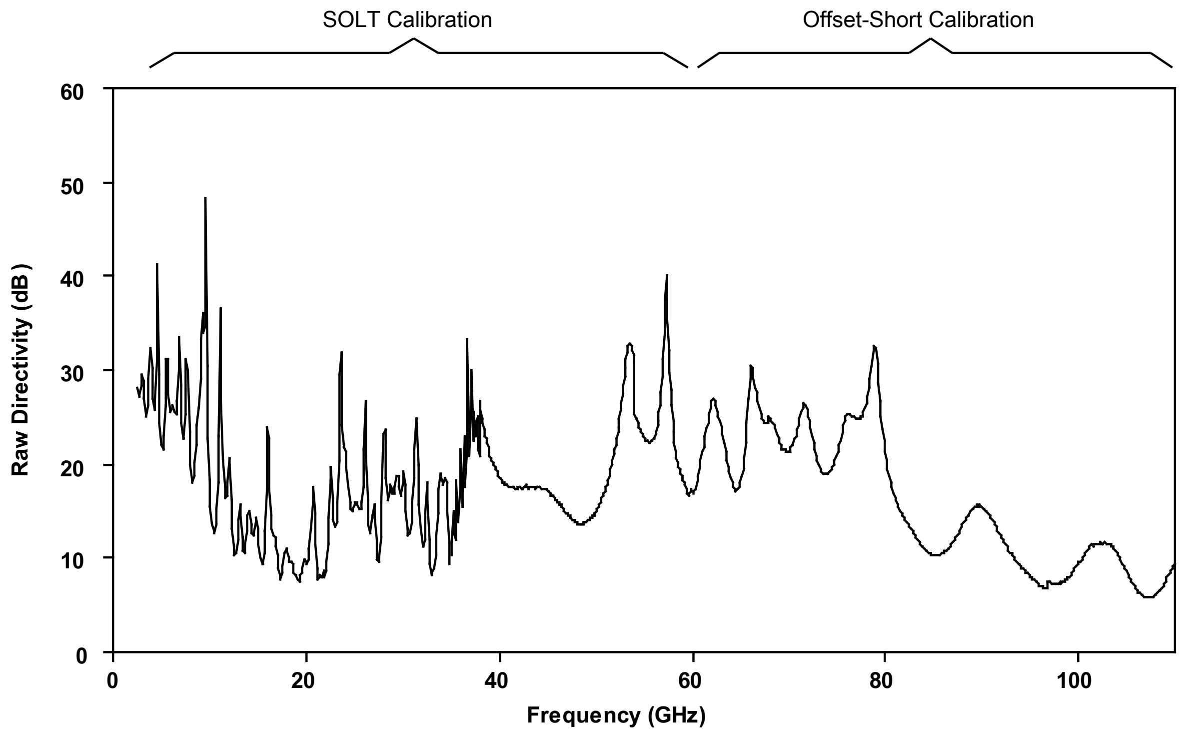

Figure 7. The measured raw directivity of the NLTL-based VNA and external reflectometer.

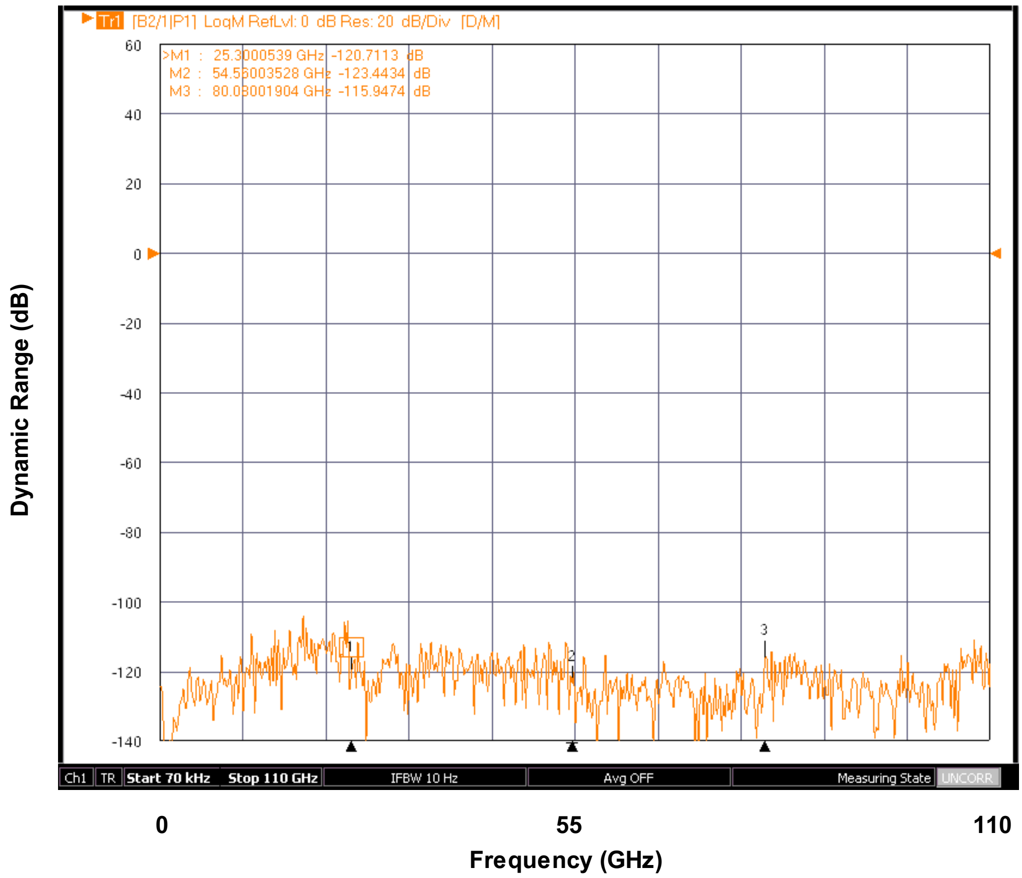

Figure 8. The measured dynamic range of the NLTL-based VNA and external reflectometers in the frequency band 70 KHz – 110 GHz at an IF bandwidth of 10 Hz. The dynamic range exceeds 100 dB in the entire band.

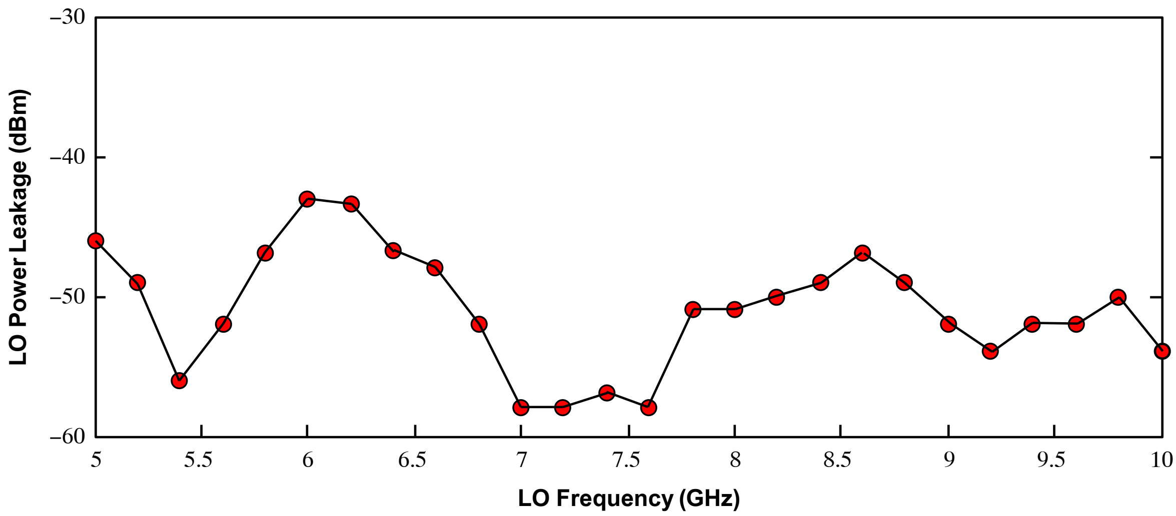

Figure 9. The measured LO leakage out of the test port of the external reflectometer in the frequency range of the LO.

V. Conclusions

In conclusion, it was shown that an NLTL-based reflectometer could be used to extend the frequency range of a VNA into the millimeter waves. Its small form factor and lightweight make it a prime candidate for use in multi-port on-wafer measurements and near-field scanning. In addition, the ability to locate the reflectometer close to a DUT enhances test-port power, and improves the VNA's raw directivity which leads in turn to long-term measurement stability.

A key advantage of the miniature reflectometer is its unobtrusive nature in that it leaves the RF path starting in the base VNA and leading to the test port intact. The end result is continuous frequency coverage demonstrated here from 70 KHz to 110 GHz, a range limited only by the bandwidth of the coaxial connector and the number of NLTL-multiplier chains. The unobtrusiveness feature, combined with an NLTL-based sampling bridge allows the frequency range of a vector network analyzer to be extended without the use of combiners, while enhancing the directivity of the analyzer [10]. This is in sharp contrast with existing VNA frequency extensions in which a large external combiner is used to concatenate two frequency bands, with the added deterioration in raw directivity and additional insertion loss

References

[1] Anritsu Co., Morgan Hill, CA, USA. Available: http://www.anritsu.com/en-US/Products-Solutions/Products/MS4640A-Series.aspx

[2] E. O. Brigham, *The Fast Fourier Transform and its Applications*, Prentice Hall, N.J., 1988, pp. 20, 74.

[3] W. M. Grove, "Sampling for oscilloscopes and other RF systems: DC through X-band," *IEEE MTT,* vol. 14, no. 12, Dec. 1966.

[4] Lightning Vector Network Analyzer, ME7808A, Anritsu Co., Morgan Hill, CA.

[5] R. Landauer, "Shock waves in nonlinear transmission lines and their effect on parametric amplification," *IBM Journal of Research*, 1960, pp. 391-401.

[6] M. J. W. Rodwell, and D. M. Bloom, "Nonlinear transmission line for generation of picosecond electrical transients," *United States Patent 5014018*, May 7, 1991.

[7] M. G. Case, *Nonlinear Transmission lines for Picosecond Pulse, Impulse and Millimeter-Wave Harmonic Generation*, Ph.D. dissertation, University of California, Santa Barbara, July 1993.
[8] R. A. Marsland, M. J. W. Rodwell, and D. M. Bloom, "Integrated coplanar strip nonlinear transmission line," *United States Patent 5256996*, Oct. 26, 1993.
[9] R. A. Marsland, M. J. W. Rodwell, and D. M. Bloom, "Gallium arsenide monolithically integrated sampling head using equivalent time sampling having a bandwidth greater than 100 GHz," *United States Patents 5267020 and 5378939*, Nov. 30, 1993 and Jan. 3, 1995, respectively.
[10] K.M. Noujeim, U.S. Pat. Appl. Serial No. 12/847,100, "Vector network analyzer having multiplexed reflectometers for improved directivity," 2010.